Bulgarian Chemical Communications, Volume 49, Special Edition K2, (pp. 128 – 133) 2017

Optimization of pepsin-assisted extraction of polysaccharides from *Cynomorium songaricum*

H. Fan[1,2], Y. Su[1], L. Wang[1], G. Chen[1,*]

[1] *School of Life Sciences, The Good Agriculture Practice Engineering Technology Research Center of Chinese and Mongolian Medicine, Inner Mongolia University, Hohhot, China*
[2] *College of Chemistry and Chemical Engineering, Inner Mongolia University, Hohhot, China*

Received August 15, 2017, Revised November 15, 2017

In this paper, the pepsin-assisted extraction of *Cynomorium songaricum* polysaccharides was investigated. The study comprised a single factor experiment design and an optimization response surface methodology using Box-Behnken design providing the optimal extraction conditions as pH of 1.5, liquid-to-solid ratio of 108:1, and proteolysis temperature of 40 °C. Under these conditions, the highest *C. songaricum* polysaccharides yield reached 23.63 ± 0.21%, which represented an increase of 233% compared to the conventional hot-water extraction. Their structures were determined *via* chemical analysis, ultraviolet spectra, Fourier-transform infrared spectra, scanning electron microscopy, and atomic force microscopy. These findings may provide a theoretical basis for further systematic research and utilization of *C. songaricum* polysaccharides resources.

Key words: Pepsin, Extraction, *Cynomorium songaricum*, Polysaccharide

INTRODUCTION

Cynomorium songaricum, is a wild perennial plant mainly parasitizing on the roots of the genera *Nitraria* which widely is distributed across the deserts of Northwestern China, Central Asia, Iran, and Mongolia [1]. In traditional Chinese medicine, *C. songaricum* is generally prescribed for reinforcing the immune system, treating lumbar weakness and enhancing sexual ability [2]. Modern chemical research revealed that polysaccharides from *C. songaricum* displayed a range of biological effects, including anti-fatigue, anti-oxidation, and hypoglycemic activity [3-5], rendering it an ideal candidate for treating senile diseases without side effects [2]. Because there were only few reports [5-7] during last decades, the development of efficient extraction and purification methods is essential to meet the increasing demand for high-quality and multi-functional *C. songaricum* polysaccharides (CSPs).

The main factor affecting the extraction yield of polysaccharides is the extraction process used. Many technologies have been discovered, including hot water extraction (HWE), microwave-assisted extraction, and bio-enzymatic method [7-9]. Among them, enzyme-assisted extraction attracted much attention due to its high efficiency and environmental compatibility overcoming the shortcomings of conventional procedures [10].

Up to now, extraction of polysaccharides from *C. songaricum* using pepsin-assisted extraction (PAE) technology has not been reported. The objective of this study was to investigate the main variables and optimize the PAE conditions using single factor experimental design and Box-Behnken design (BBD) [11,12]. Moreover, the characteristics of CSPs-PAE and CSPs-HWE were determined by chemical composition analysis, UV, FT-IR, SEM and AFM analysis. These data will lay a foundation for future pharmacological and biochemical studies of CSPs.

EXPERIMENTAL

Materials and chemicals

Fresh *C. songaricum* stems were collected in a marginal zone of Hobq Desert, Inner Mongolia, China. The voucher specimen was kept in the Herbarium of Inner Mongolia University. Pepsin (≥1200.0 U/g) was obtained from Sinopharm Chemical Reagent Co., Ltd. All other reagents were of analytical grade.

PAE procedure

C. songaricum powder (100 g) was infused in triplicate by dichloromethane:methanol (2:1) at room temperature for 12 h to remove lipids and colored materials. After the defatted powder was hydrolyzed in a thermostatic oscillator vibrator (Electron 420, Thermo Co., USA) using pepsin at certain conditions, the sample was rapidly heated in boiling water and refluxed for a designated time. The mixture was centrifuged, and the supernatant was deproteinated using the Sevag reagent. Then, it was concentrated, precipitated and lyophilized to obtain

To whom all correspondence should be sent:
E-mail: guilinchen61@163.com

crude polysaccharides, labelled as CSPs-PAE. The CSPs yield (%) resulting from the extraction was calculated using the equation below:

$$\text{CSPs yield}(\%) = \frac{\text{weight of dried crude CSPs(g)}}{\text{weight of samples(g)}} \times 100\% \quad (1)$$

Hot water extraction (HWE) of CSPs was performed as a control experiment.

Single factor experimental design

The ranges of proteolysis pH (pH), proteolysis temperature (PTe), proteolysis time (PTi), extraction time (ET), pepsin concentration (PC) and liquid-to-solid ratio (LS) were studied using a single factor design. The levels of each factor are given in Table 1. One factor was changed with the other factors remaining constant in each experiment. The effect of each factor was evaluated by the resulting CSPs yield.

Table 1. The levels of each factor used in the single factor experimental design.

Level	Factors					
	pH	PTe(°C)	PTi(h)	ET(min)	PC(%)	LS(V/w)
1	1.0	30	3	10	0.5	30:1
2	1.5	35	4	30	1.0	50:1
3	2.0	40	5	60	1.5	70:1
4	2.5	45	6	90	2.5	100:1
5	3.0	50	7	120	4.0	140:1

Box-Behnken design (BBD)

Based on the preliminary study, a three-factor and three-level BBD (Design-Expert software, version 8.0.6.1, USA) was used to determine the optimal conditions for PAE of CSPs. The levels of each factor and the design matrix are given in Table 2. The extraction yield was taken as the response. The low, middle, and high levels of each variable were coded as -1, 0, and 1, respectively.

Chemical composition analysis

The polysaccharide content of the CSPs was evaluated using the phenol-sulfuric acid method with glucose as the standard [13]. Protein content was measured by the Bradford method [14] with bovine serum albumin as the standard.

Ultraviolet spectra (UV) and Fourier-transform infrared spectra (FT-IR)

The samples (CSPs-PAE and CSPs-HWE) were dissolved and diluted to a proper concentration and scanned from 200 to 400 nm with the UV-vis spectrophotometer (TU-1901, Purkinje General Instrument, China). The FT-IR spectrum was detected on a Nicolet 6700 spectrometer (Thermo Co., USA) using KBr disk method in the frequency range of 400 - 4000 cm^{-1} [15].

Atomic force microscopy analysis (AFM)

The polysaccharides were dissolved in deionized water at 100 μg/mL. 10 μL of the solution was deposited onto a freshly cleaved mica surface and allowed to dry at room temperature. Meanwhile, a filter paper was placed at the end of the mica to remove excessive solution [16]. Atomic force microscopy (AFM) was performed in intermittent contact mode with a scanning probe microscope (CSPM5500, Benyuan Nano Co., China).

Scanning electron microscopy analysis (SEM)

The sample particles were coated with a thin layer of gold under reduced pressure. The shape and surface characteristics were determined using field-emission SEM (FESEM, S-4800, Hitachi, Japan).

RESULTS AND DISCUSSION

Single factor analysis of PAE

Plant cell wall consists of a rigid skeleton of cellulose and glycoprotein. Pepsin treatment was able to cleave specifically at the telopeptide region of glycoprotein from the cell wall [17]. The effects of several parameters were proven to be critical to the yield of the PAE procedure, such as pepsin activity, extraction time and liquid-to-solid ratio. Hence, we designed a five-level single factor analysis to assess their optimum scope and the results are summarized in Figure 1.

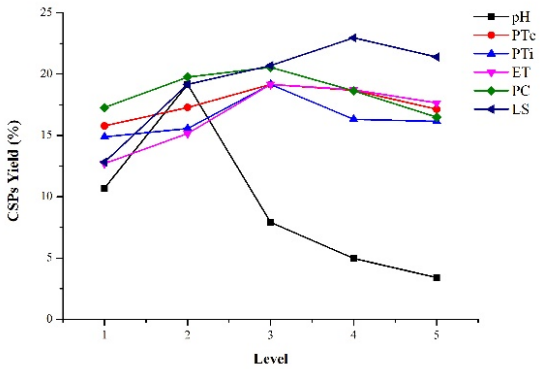

Fig. 1. Effect of pH, PTe, PTi, ET, PC and LS on the yield of CSPs. PTe, proteolysis temperature; PTi, proteolysis time; ET, extraction time; PC, pepsin concentration; LS, liquid-to-solid ratio.

In the single factor experiments, maximum CSPs yield was obtained with the following levels: pH level 2; proteolysis temperature level 3; proteolysis time level 3; extraction time level 3; pepsin concentration level 3; and liquid-solid ratio level 4.

In other words, the optimum conditions were as follows: pH, 1.5; proteolysis temperature, 40 °C; proteolysis time, 5 h; extraction time, 60 min; pepsin concentration, 1.5%; and liquid-to-solid ratio, 100:1.

Box-Behnken design and analysis for model fitting

A 17-run BBD was utilized to optimize the three independent variables (X_1: proteolysis pH, X_2: liquid-solid ratio, and X_3: proteolysis temperature). Table 2 shows the layout and the corresponding results obtained with each run. Based on the analysis of multiple regressions, the resulting quadratic polynomial equation was as follows:

$$Y = 22.82 + 1.84X_1 + 0.30X_2 + 0.74X_3 - 0.20X_1X_2 - 0.13X_1X_3 + 0.47X_2X_3 - 3.53X_1^2 - 0.96X_2^2 - 0.037X_3^2 \quad (2)$$

Analysis of variance (ANOVA) study was used to evaluate the impact and significance of each term (linear terms, squared terms and interactions) in the regression equation, and results are summarized in Table 3. The *F*-value of 173.65 suggested that the model is highly significant at $P < 0.0001$. The adjusted determination coefficient (Adj-R^2) of 0.9898 confirmed that the model was significant. A low coefficient of variation (CV) of 1.17% clearly indicated a high degree of precision and good reliability of the experimental values. In this research, the lack of fit *F*-value and *P*-value were found to be 2.78 and 0.1741, respectively, which indicated that the model was sufficiently accurate for predicting the relevant response.

Additionally, the two linear coefficients (X_1 and X_3), two quadratic coefficients (X_1^2 and X_2^2), and one interactive coefficient (X_2X_3) have extremely high significance ($P < 0.01$) to explain the individual effects of proteolysis pH and temperature and the

Table 2. Design and results for BBD.

Run	Coded variable levels			CSPs yield (%)	
	pH (X_1)	LS (X_2, V/m)	PTe (X_3, °C)	Experimental	Predicted
1	(1.4) 0	(80:1) -1	(40) 1	21.90	21.80
2	(1.0) -1	(100:1) 0	1	18.26	18.28
3	0	(120:1) 1	(30) -1	20.81	20.91
4	(1.8) 1	-1	(35) 0	19.83	20.07
5	1	1	0	20.34	20.26
6	0	1	1	23.12	23.34
7	1	0	1	21.84	21.70
8	-1	1	0	17.23	16.99
9	0	-1	-1	21.47	21.25
10	-1	0	-1	16.41	16.55
11	1	0	-1	20.49	20.47
12	-1	-1	0	15.91	15.99
13	0	0	0	23.01	22.82
14	0	0	0	22.83	22.82
15	0	0	0	22.95	22.82
16	0	0	0	22.54	22.82
17	0	0	0	22.78	22.82

Table 3. Analysis of the variance (ANOVA) for the fitted quadratic polynomial model.

Source	Sum of squares	d*f*	Mean square	*F*-value	*P*-value	Significance
Model	91.71	9	10.19	173.65	<0.0001	**
X_1	26.97	1	26.97	459.69	<0.0001	**
X_2	0.71	1	0.71	12.17	0.0102	*
X_3	4.41	1	4.41	75.16	<0.0001	**
X_1X_2	0.16	1	0.16	2.80	0.1385	
X_1X_3	0.063	1	0.063	1.07	0.3364	
X_2X_3	0.88	1	0.88	15.06	0.0060	**
X_1^2	52.61	1	52.61	896.54	<0.0001	**
X_2^2	3.88	1	3.88	66.09	<0.0001	**
X_3^2	5.842E-3	1	5.842E-3	0.100	0.7616	
Residual	0.41	7	0.059			
Lack of fit	0.28	3	0.093	2.78	0.1741	
Pure error	0.13	4	0.033			
Cor. Total	92.12	16				
	R^2 = 0.9955		Adj-R^2 = 0.9898		CV% = 1.17	

*Significant at $P < 0.05$, **Significant at $P < 0.01$.

interaction effect of liquid-to-solid ratio and proteolysis temperature on the extraction yield of CSPs. The linear coefficient (X_2) was significant ($P < 0.05$), which means that the liquid-to-solid ratio was also an important independent variable. The other term coefficients were insignificant ($P > 0.05$).

Optimization of the procedure

The 3D response surfaces and 2D contour plots were generated based on the regression equation 2, providing a visual interpretation of the interactions between variables, as well as the relationships between CSPs yields and the experimental levels of each variable, as presented in Figure 2. An elliptical or saddle contour plot indicates significant interactions between the corresponding variables while a circular contour plot implies otherwise. In this work, the mutual interactions between the three independent variables (proteolysis pH, proteolysis temperature, liquid-to-solid ratio) were all significant.

Figures 2A and 2D, which fixed the proteolysis temperature at level 0, show that the CSPs yield increased with increasing proteolysis pH (X_1) and liquid-to-solid ratio (X_2) from 1 to 1.5 and 80:1 to 108:1, respectively. At this fixed temperature (0 level), the maximal CSP yield was 23.01%. The plots based on varying pH (X_1) and temperature (X_3) are shown in Figures 2B and 2E, while liquid-to-solid ratio was kept constant at the central point of design. Figures 2C and 2F present that the CSPs yield increased with liquid-to-solid ratio from 80:1 to 108:1. When the pH was fixed at 1.5, a medium liquid-to-solid ratio and moderate proteolysis temperature were good for the CSPs yield.

Verification of predictive model

The predicted optimum values of the tested variables were 1.5 for proteolysis pH, 108:1 for liquid-to-solid ratio, and 40 °C for proteolysis temperature. This set of conditions was used to experimentally validate and predict the values of the responses using the model equation. Under the optimal conditions, the extraction yield of CSPs was 23.63 ± 0.21% (N = 3), which was not significantly different ($P > 0.05$) from the predicted value of 23.86%. This indicated that the model designed in this study was adequate for the extraction process.

Comparison of HWE and PAE

The CSPs yields obtained using HWE and PAE were 7.10 ± 1.23% and 23.63 ± 0.21%, respectively. Thus, the application of PAE positively affected the CSPs yield. Under the optimal conditions for PAE, the CSPs yield increased by 233% compared to the conventional HWE method.

Chemical composition analysis

The crude CSPs were preliminarily characterized using chemical analysis. The contents of

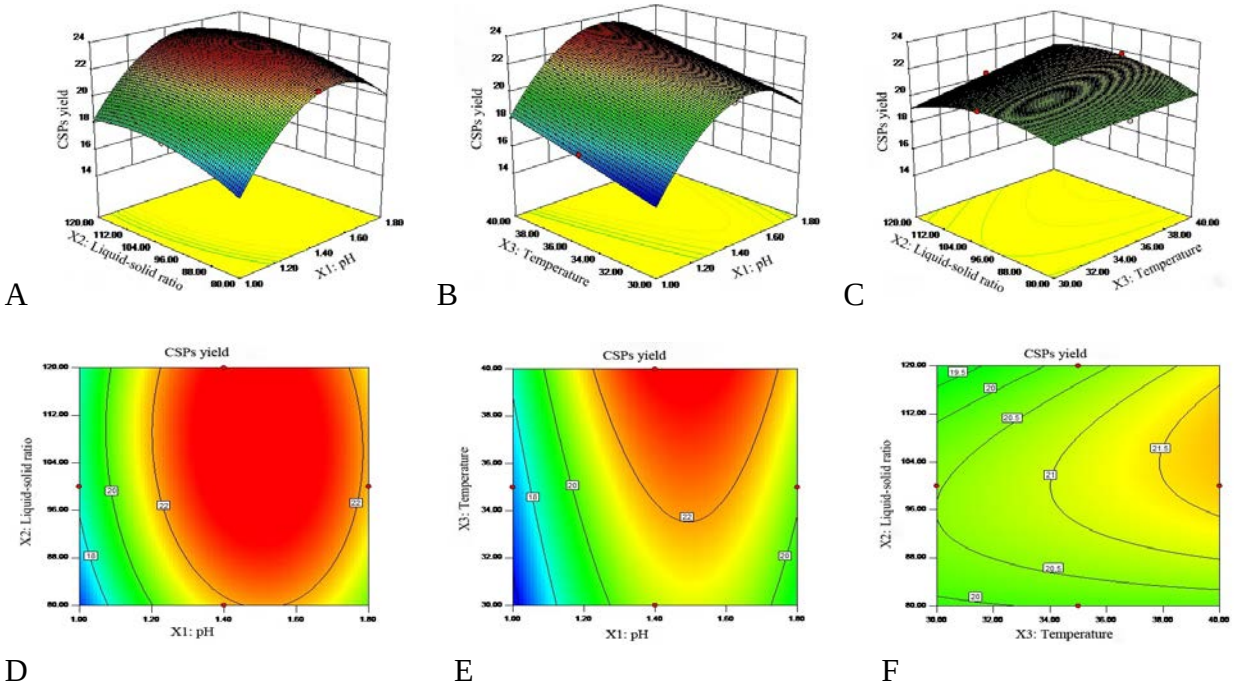

Fig. 2. Response surface plots (A, B, and C) and contour plots (D, E, and F) showing the effects of the interaction of proteolysis pH, liquid-solid ratio, and proteolysis temperature on the response of CSPs yield.

polysaccharide and protein in CSPs-PAE were 90.63 ± 0.77% and 1.07 ± 0.19%, respectively. In the control (HWE), the corresponding contents of CSPs were 71.73 ± 0.64% and 7.57 ±0.28%.

UV and FT-IR analysis

The UV spectra of CSPs-HWE showed strong absorbance at about 200 nm and medium absorbance at 280 nm, indicating the involvement of protein which is consistent with the relatively higher protein contents obtained by chemical analysis. No apparent UV absorption peak was observed around 280 nm in the spectrum of CSPs-PAE, suggesting that the protein content of the sample was negligible.

The FT-IR spectra of CSPs-PAE and CSPs-HWE are shown in Figure 3, which displays a similar trend but differentiates in details.

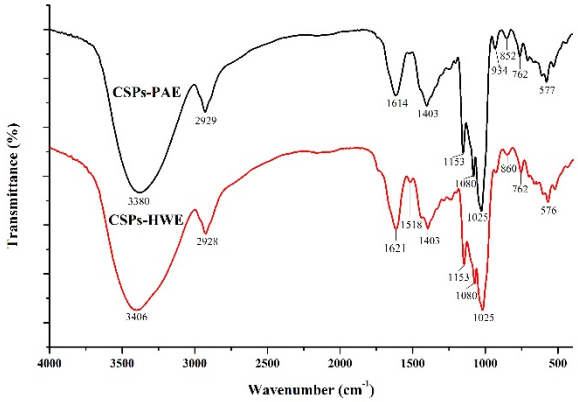

Fig. 3. UV (A) and FT-IR (B) spectra of CSPs-HWE and CSPs-PAE.

Both CSPs-HWE and CSPs-PAE exhibited absorption bands of O-H at 3400 - 3500 cm^{-1}, C-H at 2900 - 3000 cm^{-1}, C-O and C-O-C at 1000 - 1200 cm^{-1}. Three peaks at 1153, 1080, 1025 cm^{-1} in the 1200-1000 cm^{-1} region indicated pyranose rings in these two samples.

In the spectrum of CSPs-HWE, the absorption band at 1518 cm^{-1} was the characteristic peak of CO-NH bending vibration [18], which was not observed in CSPs-PAE. This result further explained the lower protein content in CSPs-PAE (1.07 ± 0.19%). The peak at 852 cm^{-1} was the absorption of α- pyranose ring [19] in CSPs-PAE. However, in the spectrum of CSPs-HWE, the peak was found at 860 cm^{-1} proving the existence of β-configuration.

AFM and SEM analysis

The surface morphology of CSPs obtained from different process and the residues after extraction were elucidated by AFM and SEM.

AFM was exploited to directly observe the chain conformation of the polysaccharides. An AFM image of CSPs-HWE (Figure 4A) shows polysaccharide chains tangling with each other and emerging as large condensed clusters. Figure 4B shows two long stretches where no clustering happens and regions where there is a clear presence of aggregation in CSPs-PAE. Some of the polysaccharide chains were nicely spread out and measured to be longer than 500 nm. The highest single polysaccharide chain can reach 6.5 nm. Compared to CSPs-HWE, CSPs-PAE was associated with lower molecular aggregation and an extended polysaccharide chain, increasing the flexibility of the molecule.

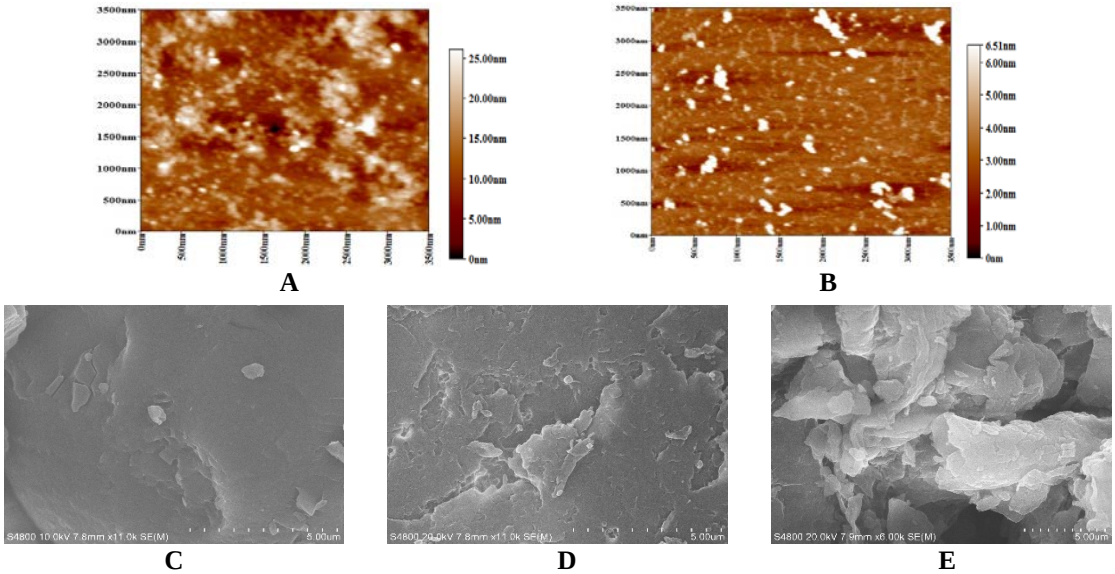

Fig. 4. Atomic force microscopy (AFM) images of CSPs obtained by HWE (A) and PAE (B). and scanning electron microscope (SEM) photographs of the raw material (C), residues after extraction by HWE (D) and PAE (E)

Figures 4C-E present the micrographs of the raw material (C), residues after extraction by HWE (D) and PAE (E), respectively. After a HWE process, little destruction of the residues microstructure occurred, while the residues resulting from PAE had large lamellae on their surfaces. This significant change is probably due to the degrading ability of pepsin rendering the intracellular materials more accessible for extraction, which contributed to the higher efficiency of polysaccharide extraction. Therefore, in the PAE process, the plant tissues were remarkably destructed, and the CSPs can be released more easily into the extraction solution than by the HWE process.

CONCLUSION

A pepsin-assisted extraction to acquire CSPs from the stem of *Cynomorium songaricum* was optimized by a 17-run BBD with response surface methodology based on single factor experiments. The second-order polynomial model gave a satisfactory description of the experimental data giving the optimum conditions as pH of 1.5, liquid-solid ratio of 108:1, and proteolysis temperature of 40 °C. Under these conditions, the highest CSPs yield was 23.63 ± 0.21% in accordance with the predicted value of 23.86% and represented 233% of that obtained by the traditional HWE method. Compared to CSPs-HWE, CSPs-PAE provided higher contents of polysaccharide (90.63 ± 0.77%), as well as lower contents of protein (1.07 ± 0.19%). Moreover, the CSPs were characterized by UV, FT-IR, SEM, and AFM which showed that CSPs-PAE differentiated from CSPs-HWE in functional groups and surface morphology leading to their distinct properties. The precise chemical structures and the unique biological functions of CSPs-PAE are currently under investigations.

Acknowledgments: *This work was kindly supported by the National Key Technology R&D of China (2011BAI07B07), Grants-in-Guide for scientific research from Science and Technology office of Inner Mongolia (2010-2013) and the Natural Science Foundation of Inner Mongolia (2015MS0212).*

REFERENCES

1. S. Jin, Eerdunbayaer, A. Doi, T. Kuroda, G. Zhang, T. Hatano, G. Chen, *J. Agric. Food Chem*., **60**, 7297 (2012).
2. Q. Chu, X. Tian, M. Lin, J. Ye, *J. Agric. Food Chem.*, **54**, 7979 (2006).
3. Z. Xiong, X. Ma, Y. Sun, C. Yao, A. Chi, W. Wang, L. Zheng, L. Li, J. Ma, M. Zhang, *J. Shaanxi Norm. Univ*., **39**, 103(2011).
4. F. Wang, Q. Liu, W. Wang, X. Li, J. Zhang, *Int. J. Biol. Macromol*., **87**, 222 (2016).
5. J. Wang, J. Zhang, B. Zhao, Y. Wu, C. Wang, Y. Wang, *Food Chem*., 120, 443 (2010).
6. G. Shi, W. Jiang, L. Cai, G. Sui, *Int. J. Biol. Macromol*., **48**, 788 (2011).
7. F. Wang, W. Wang, Y. Huang, Z. Liu, J. Zhang, *Food Hydrocolloid*., **47**, 79 (2015).
8. K. Zhong, W. Lin, Q. Wang, S. Zhou, *Int. J. Biol. Macromol*., **51**, 612 (2012).
9. M. Puri, D. Sharma, C.J. Barrow, *Trends Biotechnol.*, **30**, 37 (2012).
10. H. Chen, X. Zhou, J. Zhang, *Carbohyd. Polym*., **111**, 567 (2014).
11. A. Zhang, X. Li, C. Xing, J. Yang, P. Sun, *Int. J. Biol. Macromol*., **65**, 28 (2014).
12. Y. Xu, F. Cai, Z. Yu, L. Zhang, X. Li, Y. Yang, G. Liu, *Food Chem*., **194**, 650 (2016).
13. M. Dubois, K.A. Gilles, J.K. Hamilton, P.A. Rebers, F. Smith, *Anal. Chem*., **28**, 350 (1956).
14. M.M. Bradford, *Anal. Biochem.*, **72**, 248 (1976).
15. Q. Xiong, X. Li, R. Zhou, H. Hao, S. Li, Y. Jing, C. Zhu, Q. Zhang, Y. Shi, *Carbohyd. Polym*., **108**, 247 (2014).
16. I. Austarheim, B.E. Christensen, I.K. Hegna, B.O. Petersen, J.O. Duus, D. Diallo, M. Inngjerdingen, B.S. Paulsen, *Carbohyd. Polym*., **89**, 259 (2012).
17. R. Mohammadi, M.A. Mohammadifar, A.M. Mortazavian, M. Rouhi, J.B. Ghasemi, Z. Delshadian, *Food Chem*., **190**, 186 (2016).
18. B.E. Abdelmalek, J. Gómez-Estaca, A. Sila, O. Martinez-Alvarez, M.C. Gómez-Guillén, S. Chaabouni-Ellouz, M.A. Ayadi, A. Bougatef, *LWT - Food Sci. Technol*., **65**, 924 (2016).
19. H. Zhang, J.Q. Wang, S.P. Nie, Y.X. Wang, S.W. Cui, M.Y. Xie, *Int. J. Biol. Macromol*., **79**, 248 (2015).